

SIMULATION OF A VARIABLE RELUCTANCE STEPPING MOTOR FOR SINUSOIDAL AND STEP EXCITATIONS

J. Faiz and R. Iranpour

*Department of Electrical Engineering
Faculty of Engineering
University of Tabriz
Tabriz, Iran*

Abstract Steady-state dynamic simulation of a variable reluctance stepping motor is carried out by applying two different excitation voltages. First a single-step voltage is applied to the motor, and a sinusoidal voltage, as the first term of Fourier series of the single-step voltage, is then used as the input voltage of the motor. In both cases plots of machine torque, current and speed are presented. A comparison between the results of the two cases shows that a sinusoidal input voltage cannot predict the real performance of the motor, and in critical dynamic conditions, a single-step response is far from the reality. Reasons for these discrepancies arising from the various factors are discussed in the paper.

Key Words Variable Reluctance Motor, Simulation, Excitation Voltage Dynamic Performance

چکیده شبیه سازی دینامیکی حالت ماندگار موتور پله ای یا مقاومت مغناطیسی متغیر با اعمال دو ولتاژ تحریک مختلف انجام می شود. ابتدا یک ولتاژ پله به موتور وارد می شود و سپس ولتاژ سینوسی بعنوان جمله اول بسط سری فوریه آن ولتاژ به عنوان ولتاژ ورودی موتور بکار می رود. در هر دو حال منحنی های گشتاور، جریان و سرعت موتور ارائه می گردد. مقایسه بین نتایج این دو حالت نشان می دهد که ولتاژ ورودی سینوسی نمی تواند عملکرد واقعی موتور را پیش بینی کند، و در شرایط دینامیکی حساس، پاسخ تک پله ای از واقعیت به دور است. دلایل این تفاوت ها که ناشی از عوامل مختلف است مورد بحث قرار می گیرد.

INTRODUCTION

A three-stack Variable Reluctance (VR) stepping motor has a stator with a number of wound salient poles. The rotor consists of toothed cylindrical soft laminated magnetic iron, the teeth of which have a relationship with the stator poles and defines the stepping angle. When the stator windings are energised, the rotor will seek a path of minimum reluctance between the salient poles and rotor. This position is stable and external torque is required to move the rotor. By proper selection of the energisation sequence, the stable points can be made to move, giving to stepped motion of the rotor.

VR stepping motor is used widely in motion control systems where it often operates in a continuous

or constant-speed mode rather than in a stepping mode. By controlling the on-time and amplitude of the input voltage, speed of the motor can be controlled. The analysis of the motor is basically difficult and requires an elaborate calculation.

Regarding the variety and numerous applications of VR stepping motors in industries, steady-state dynamic simulation of these motors is necessary. Researchers have used different methods to predict the performance of the motors [1-4]. One of these methods in which a single-step voltage is used as an input [5], the first term of its Fourier series is left for a further study of the motor. The results have been compared with those obtained using average-value model, and it has been concluded that the latter model cannot accurately predict the steady-state dynamic

behaviour of the motor.

Steady-state dynamic performance of a VR stepping motor applying a single-step and sinusoidal input voltages has not yet been compared. Therefore, in this paper, operation of the motor using both excitation voltages is first described and the motor is then simulated for the two excitation voltages. Finally the simulated results are compared and a proper excitation for the performance prediction is suggested.

OPERATION WITH DIFFERENT INPUT VOLTAGES

A 3-phase, three-stack VR stepping motor with two rotor teeth and six stator teeth, shown in Figure 1, is considered for this study. When rotor of the motor is placed in a magnetic field, the exerted force pulls the rotor to the region with strong magnetic field. It means that the salient pole of the rotor is moved in such a direction that the reluctance of the magnetic path tends to a minimum value. In fact, when a voltage is applied to the stator winding, the rotor pole inclines to be aligned with the produced magnetic field. If the windings in stacks a, b and c in Figure 1 are excited in turn, the rotor moves from one mini-

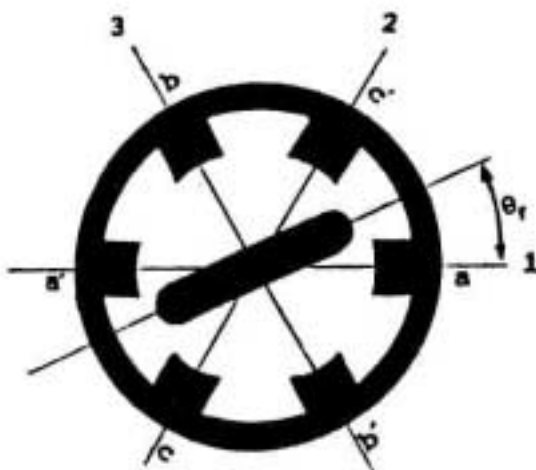


Figure 1. Schematic of three-stack VR motor.

imum reluctance position to another. Speed of rotor can be controlled by changing the conducting angle and the amplitude of the phase voltage.

Single-step voltage input

Suppose that the rotor is at the position shown in Figure 1 and axis 1 is taken to be the reference (θ_r is also defined in Figure 1). Suppose further that phase a of the motor is excited, and phases b and c have no excitation. The rotor moves and its axis coincides with axis 1; in this position $\theta_r=0$ and reluctance is minimum. For $\theta_r=\pi$, the reluctance is also minimum. Therefore the motor's inductance will be modeled as:

$$L = A + B \cos 2\theta_r \quad (1)$$

where A is the average inductance and B is the difference between the average and maximum inductances of the winding. Obviously at $\theta_r = \pi/2$, L will be minimum.

It is now assumed that the current flowing in stack a is shut off, and at the same time, a current is made flow in the windings of stack c. In this case the rotor moves to the opposite direction and becomes aligned with axis 2. When the rotor approaches axis 2, winding b is excited and excitation of winding c is removed and it is aligned with axis 3 and, therefore, the rotor rotates continuously. The position of the rotor determines the excitation sequence and this position depends on the rotor speed.

The angle between successive axes is 60 degrees and phases a, b and c are placed on the axis. If the rotor moves from $\theta_r=0$ to $\theta_r=2\pi$, it rotates one complete cycle, and for such a movement, each phase must be only excited for 120 degrees. Phase difference of the phases is also 120 degrees. Therefore, each phase must have a square-wave pulse excitation whose period (T_{puls}) can be calculated as follows

$$T_{puls} = 2\pi/\omega_r \quad (2)$$

where ω_r is angular speed of the rotor. Conducting period of each phase will be $T_{\text{puls}}/3$. It is clear that the frequency of applied voltage must be controlled on the basis of the rotor position, and input voltage is changed with frequency.

The motor is digitally controlled. It means that different positions of the rotor must be determined by a binary address. As the number of distributed binary numbers in a complete rotation becomes larger, the control of the input voltage will be more precise and the error will be less. By ignoring this error, it can be assumed that the input voltage frequency depends on the rotor frequency.

Sinusoidal voltage input

When the first term in the Fourier series for a square-wave voltage waveform is taken into account, the model is referred to as "detailed model" [5]. For phase a one can have

$$V_a = 2V_{\text{base}} \cos \omega_s t / 2\pi \quad (3)$$

where ω_s is the frequency of the applied voltage. It is assumed that the motor transient is over and angular speed is approximately equal to the synchronous angular speed, ω_s . The frequency of the rotor depends upon the power supply frequency.

MOTOR EQUATIONS

The voltage equation for a phase of the motor is

$$V = Ri + d\psi/dt \quad (4)$$

where $L = \psi/i$ has been given by Equation 1. The similar equations can be obtained for remaining stacks by a simple change of variables.

These equations can be converted into dq model equations as follows

$$V_{dq0} = CV_{abc} \quad (5)$$

where abc refer to motor quantities and voltages transformed to the dq reference frame are identified by the d_{q0} subscript. Connection matrix C is

$$[C] = \frac{2}{3} \begin{bmatrix} \sin \theta_r & \sin (\theta_r - 2\pi/3) & \sin (\theta_r - 4\pi/3) \\ \cos \theta_r & \cos (\theta_r - 2\pi/3) & \cos (\theta_r - 4\pi/3) \\ 1/2 & 1/2 & 1/2 \end{bmatrix} \quad (6)$$

The voltage matrix is

$$V_{dq0} = [M] I_{dq0} + [N] dI_{dq0}/dt \quad (7)$$

Matrices M and N may be determined using the above equations [6]. Thus

$$dI_{dq0}/dt = [N]^{-1} V_{dq0} + [N]^{-1} [M] I_{dq0} \quad (8)$$

Torque equation is as follows

$$T_e = I_{dq0}^T [C]^{-1} \partial LC^{-1} I_{dq0} / \partial \theta_r / 2 \quad (9)$$

If Equation 9 is expanded, the following result is obtained

$$T_e = 3B (i_q i_d + 2i_q i_0 \sin 3\theta_r - 2i_d i_0 \cos 3\theta_r) / 2 \quad (10)$$

Equation 10 contains terms in which i_0 is modulated by terms involving $\sin 3\theta_r$, $\cos 3\theta_r$. These will produce components of torque which are at dc and six harmonic. The third harmonic current in i_0 interacts with terms that vary sinusoidally with $3\theta_r$, to produce an average value and a six harmonic variation. Speed equation is as follows

$$d\omega_r/dt = (T_e - T_m) / J - B\omega_r / J \quad (11)$$

The above system of equations can be solved using Runge-Kutta method by choosing proper initial values.

DYNAMIC OF THE MOTOR

A VR stepping motor with maximum speed 1660 rpm and rating voltage 120 volts is simulated as an illustrative example. Per phase single-step and sinusoidal voltages at 1660 rpm is shown in Figure 2. By solving the above system of differential equations for no load and on load and then unloading conditions, theoretical steady- state dynamic responses for the motor are determined.

Figures 4, 6 and 8 display current, torque and rotor angular speed/time characteristics for the motor with sinusoidal excitation. Figures 3, 5, and 7 show the similar characteristics for the motor with a single-step excitation. No load characteristics are shown in Figures 3-6. Figures 7 and 8 present the performance characteristics of the on load motor. Figures 3 and 4 have been obtained for interval between 10 and 10.1 seconds, in which there is a large difference between the two. Figures 5 and 6 show the similar characteristics for interval between 10 and 11 seconds. Mean values and current variations are summarized in Table 1. From this table it is observed that for a single-step excitation, the mean I_q current is 0.7 A and I_q varies between 0.35A and 1.05A.

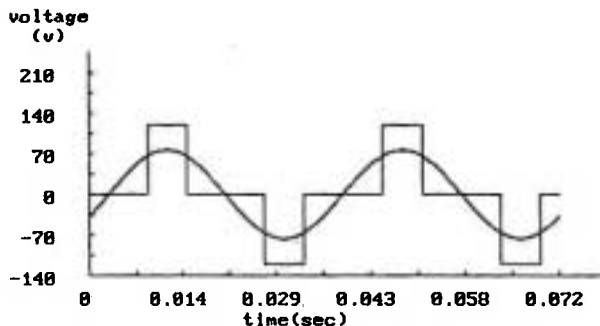


Figure 2. Input voltage waveforms.

TABLE 1. Comparison of Motor No-load Currents and Speed.

Currents & speed	Type of excitation	
	Single-step	Sinusoidal
I_q (A)	0.70 + 0.35	0.275 + 1.25
I_d (A)	-3.56 + 0.10	3.500 + 0.25
I_b (A)	0.00 + 1.00	0.000 + 0.55
w_r (rad/s)	174 + 1.4	172 + 12.00

TABLE 2. Speed and Torque Variations of the on Load Motor.

Torques & speed	Excitation voltage	
	Single-step	Sinusoidal
Speed (%)	90%	172 (rad/s) + 6%
Torque (%)	5%	14%

At $t=11s$, a load $T_m = 0.025 Nm$ is applied to the motor and variations of current and torque caused by the load are shown in Figures 7 and 8 for different excitations. The speed and torque variations are summarized in Table 2. In Figure 8d, it can be seen that the speed falls from 174 rad/s to 157 rad/s, but there is no sensible variation in Figure 7d.

COMPARISON OF THE RESULTS

Figure 8d illustrates the reduction of rotor speed from 174 rad/s to 157 rad/s. The applied torque was $T_m = 0.025 Nm$, and conducting angle of each phase was 120 degrees. Since by loading the motor, the control system cannot increase the conducting angle and adjust the speed, the speed decreases. Figure 7d does not show a considerable change, because the speed of the rotational field is w_s ; in fact, rotor rotates with synchronous speed and loading does not change other characteristics of the motor. If electric torque cannot provide the required load torque, the motor becomes unstable.

Sinusoidal voltage applied to one phase begins from zero and gradually (and continuously)

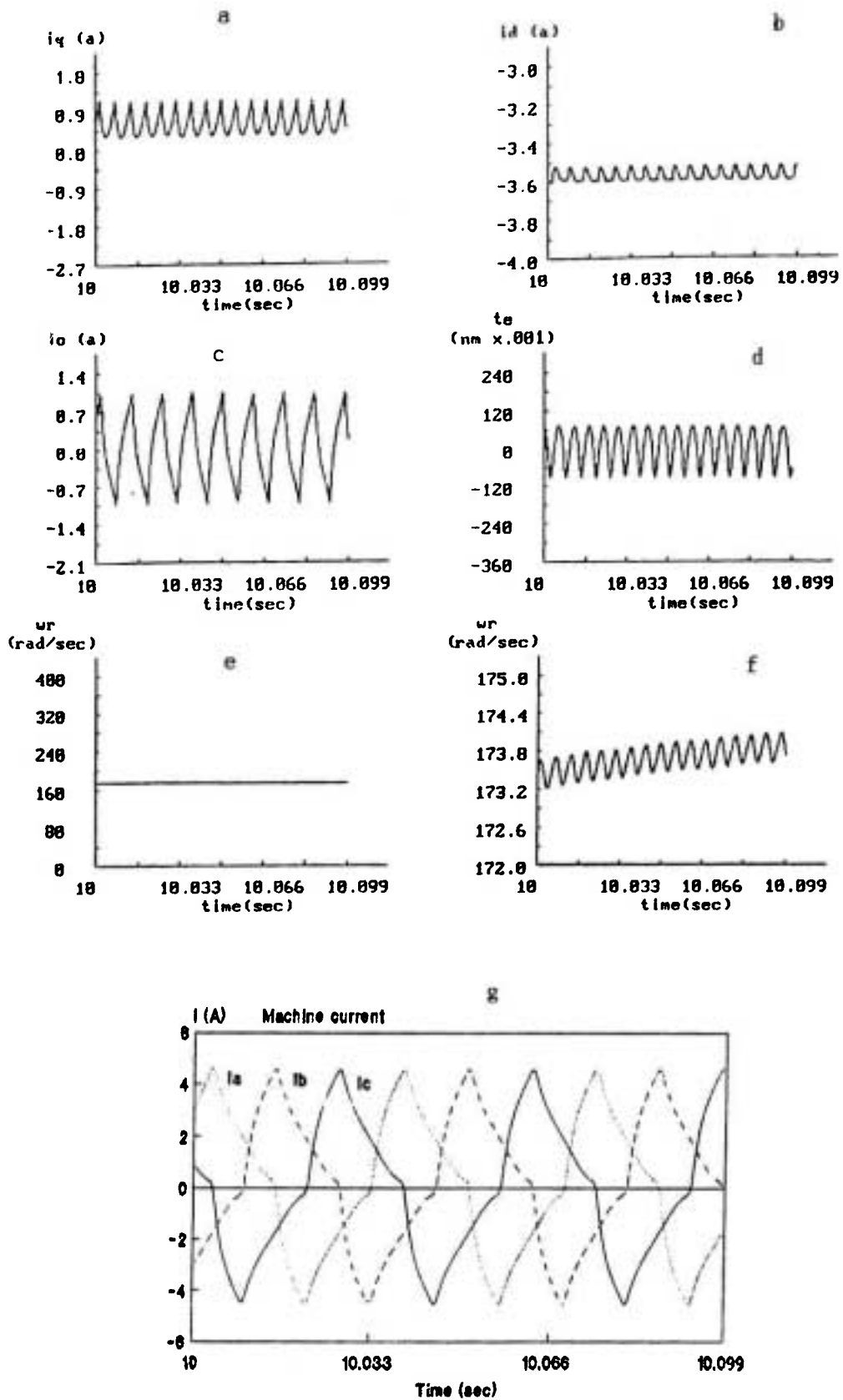


Figure 3. No load characteristics of the machine for a square-wave excitation voltage (expanded time scale).

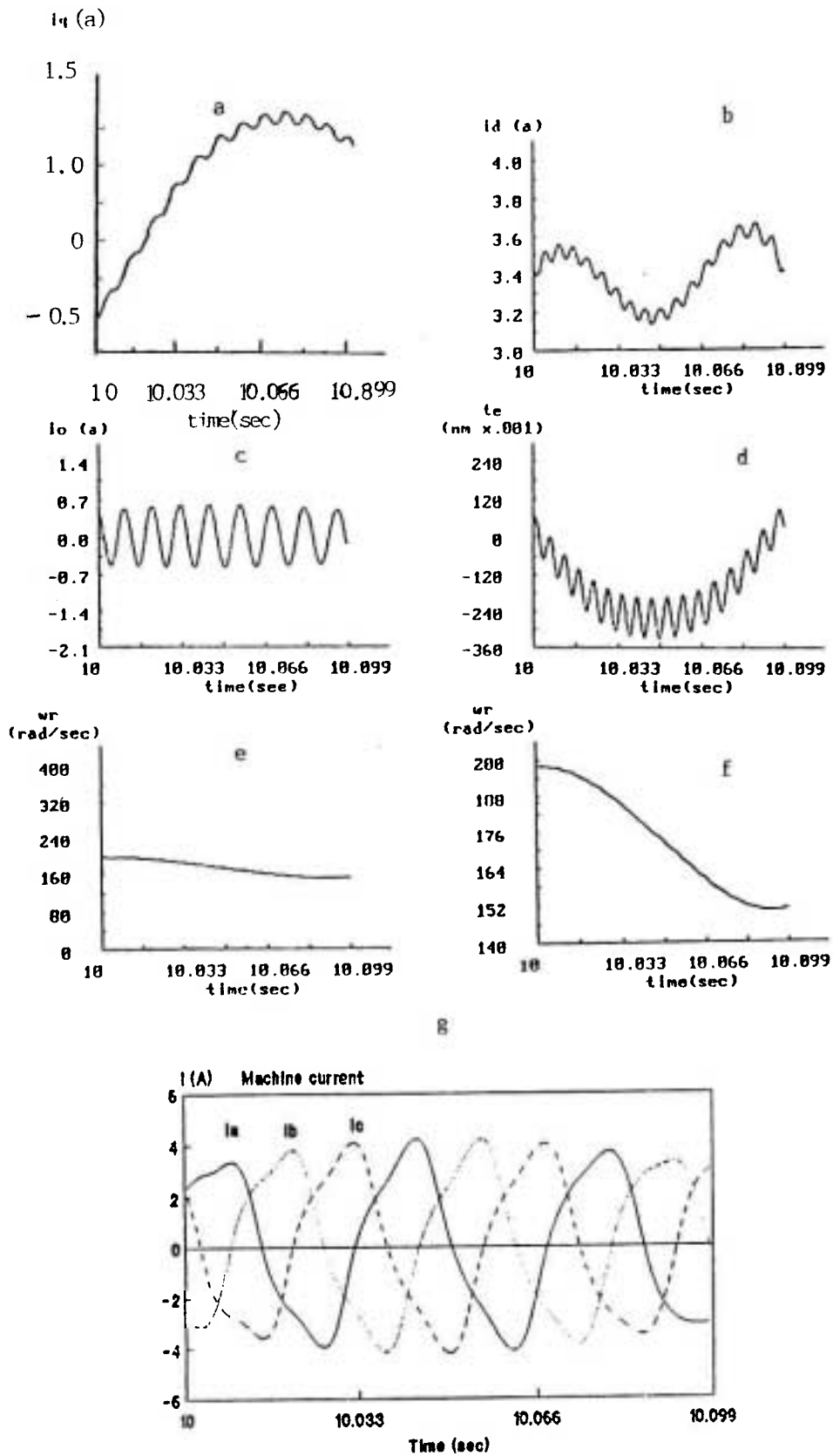


Figure 4. No load characteristics of the machine for a sinusoidal-wave excitation voltage (expanded time scale).

increases up to the maximum value and then it decreases. Such a variation produces a 6th harmonic causing oscillation in Figures 4a,b,c. This harmonic also appears in the torque equation and its influence is represented in Figures 5c, 5d, 6c and 6d.

High frequency oscillations shown in Figures 3a, b and 4a, d, resulted from frequency of the applied voltage. The ratio of rms value of the single-step voltage and sinusoidal voltage is approximately 1.2, which itself causes change of these quantities.

To clarify the influence of the excitation voltages on the equations used, Equations 5-6 are employed as follows

$$V_d = 2(V_a \sin \theta_r + V_b \sin (\theta_r - 2\pi/3) + V_c \sin (\theta_r - 4\pi/3))/3 \quad (12)$$

$$V_q = 2(V_a \cos \theta_r + V_b \cos (\theta_r - 2\pi/3) + V_c \cos (\theta_r - 4\pi/3))/3 \quad (13)$$

$$V_0 = 2(V_a/2 + V_b/2 + V_c/2)/3 \quad (14)$$

where V_a , V_b and V_c are sinusoidal or single-step voltages. For a single-step voltage, the phase of a voltage is as follows

$$V_a = f(\theta_r) = \begin{cases} V_{base} & \dots -\pi/6 < \theta_r < \pi/6 \\ 0 & \dots \pi/6 < \theta_r < 5\pi/6 \\ -V_{base} & \dots 5\pi/6 < \theta_r < 7\pi/6 \\ 0 & \dots 7\pi/6 < \theta_r < 11\pi/6 \end{cases} \quad (15)$$

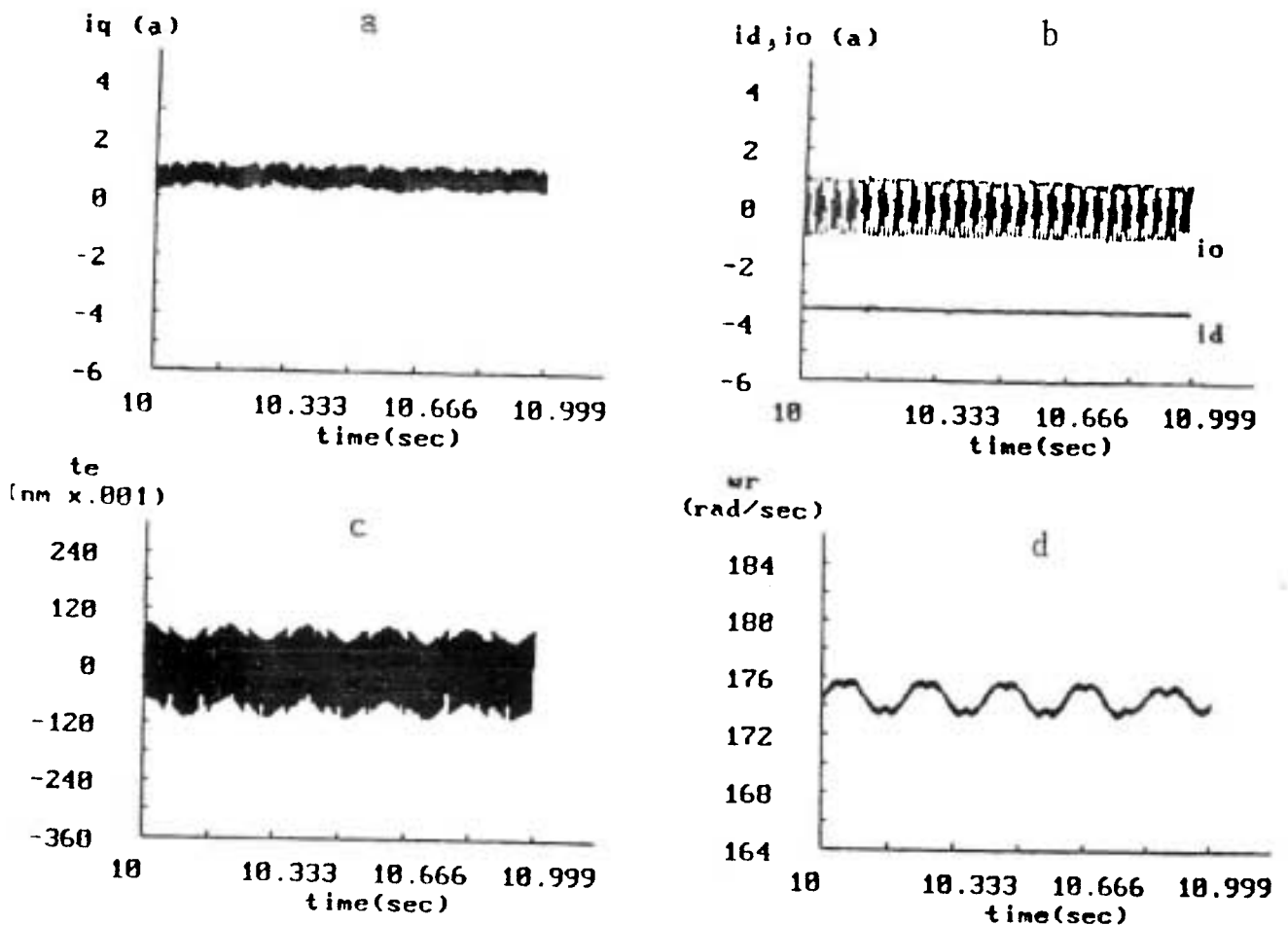


Figure 5. No load characteristics of the machine for a square-wave excitation voltage.

for b and phase c

$$V_b = f(\theta_r - 2\pi/3)$$

$$V_c = f(\theta_r - 4\pi/3) \quad (16)$$

By substituting Equations 15-16 into Equations 12-14

$$V_d = 2(-1)^m V_{base} |\sin(\theta_r - 2m\pi/3)|/3$$

$$V_q = 2(-1)^m V_{base} |\cos(\theta_r - 2m\pi/3)|/3$$

$$V_o = (-1)^m V_{base}/3 \quad (m = \text{number of stacks}) \quad (17)$$

where $m\pi/3 < \theta_r < (m+1)\pi/3$.

For sinusoidal voltages:

$$V_a = 2V_{base} \cos(\omega_s t)/\pi$$

$$V_b = 2V_{base} \cos(\omega_s t - 2\pi/3)/\pi$$

$$V_c = 2V_{base} \cos(\omega_s t - 4\pi/3)/\pi \quad (18)$$

and

$$V_d = 2V_{base} \sin(\theta_r - \omega_s t)/\pi$$

$$V_q = 2V_{base} \cos(\theta_r - \omega_s t)/\pi$$

$$V_o = 0 \quad (19)$$

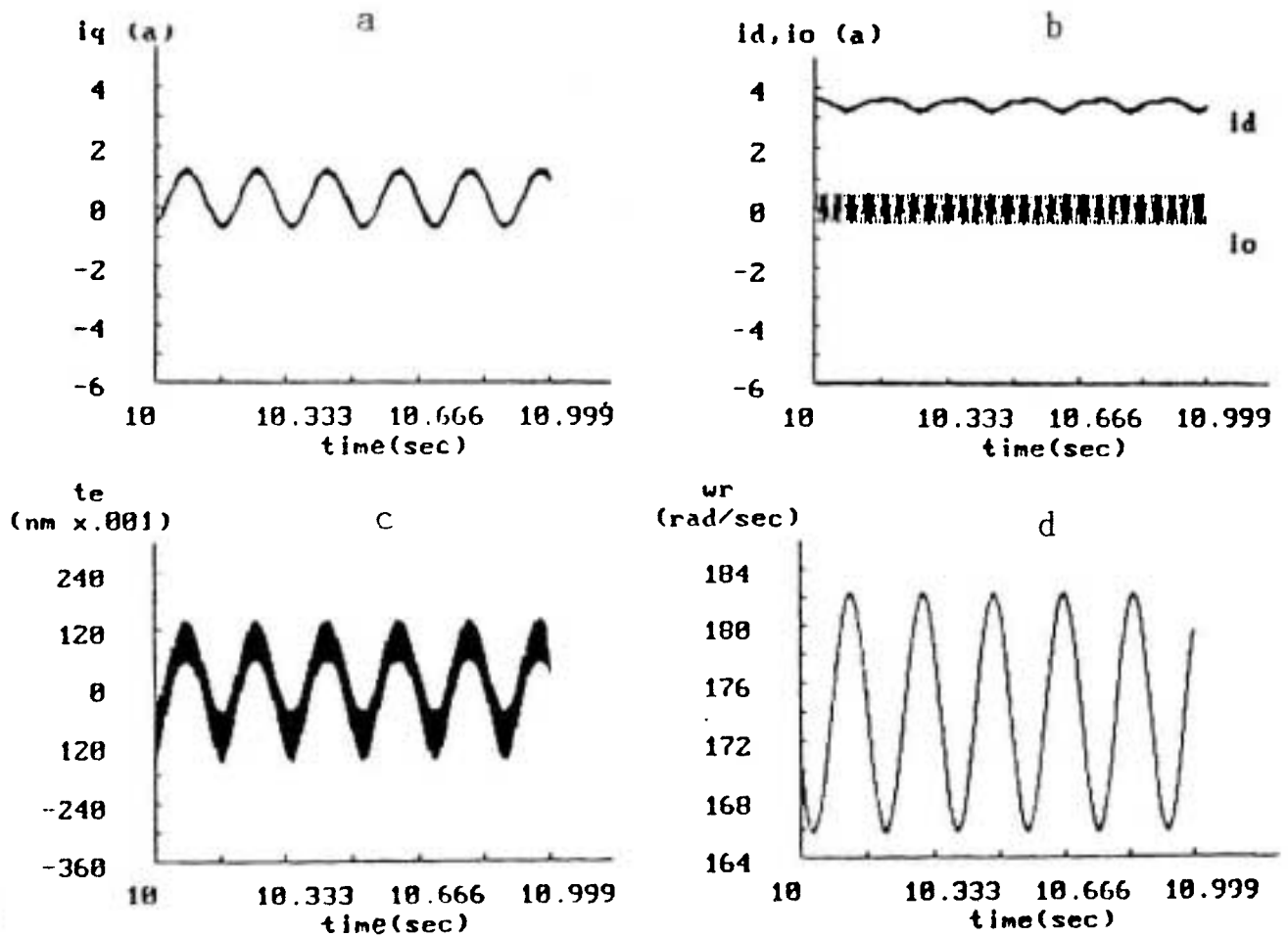


Figure 6. No load characteristics of the machine for a sinusoidal-wave excitation voltage.

Equations 17-19 present phase voltages for the sinusoidal excitation. In Equation 17, voltages are independent of speed w_s and depend upon m and θ_r . In the system of Equations 19, voltages depend on θ_r and w_s . Evidently when these voltages are substituted in Equation 8, different solution will be obtained and no load and on load conditions will not be identical. When motor is loaded (Figure 9), at $t=12s$, the period of the pulse and sinusoidal waveforms are different. Conducting angle of each phase is 120 degrees for the square-waveform and its period is increased by the reduction of the speed. Consequently, the frequency of the step wave input is changed, whereas frequency of sinusoidal wave is not changed so much.

CONCLUSIONS

In the present paper the steady-state dynamic performance of a VR stepping motor for two different excitation voltages, square-wave and sinusoidal-wave, was studied. Variations of the current, torque and speed versus time were determined for both excitations and they were compared. It was found that in some cases, using a sinusoidal voltage instead of a square-wave voltage is not convenient for prediction of the proper performance of the motor. This is particularly true when control of the speed is required. In such a case, using the sinusoidal waveform as the first term of the Fourier series of the square-wave voltage does not suffice and produces error in

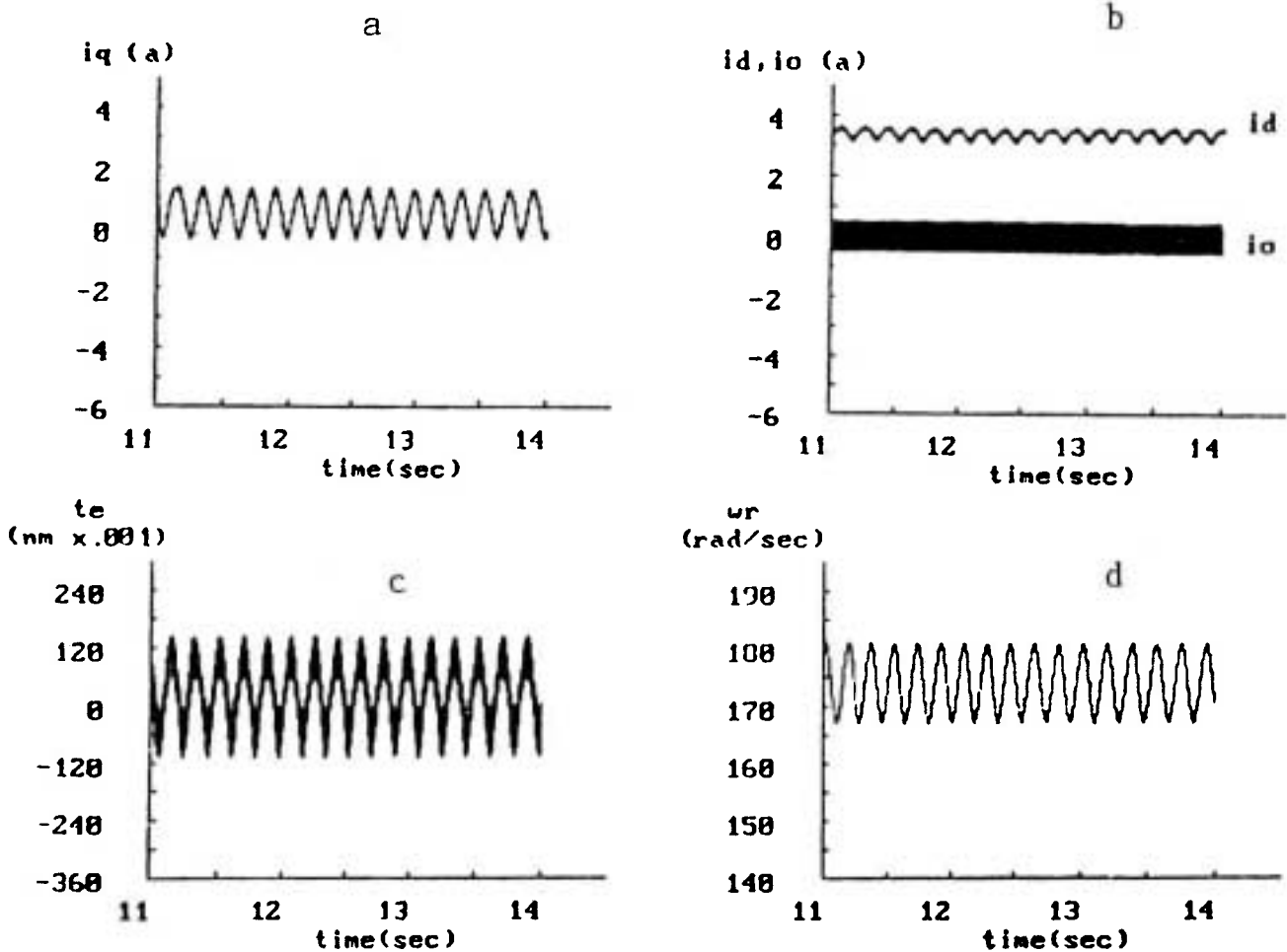


Figure 7. Steady-state on load performance of the machine for a square-wave excitation voltage.

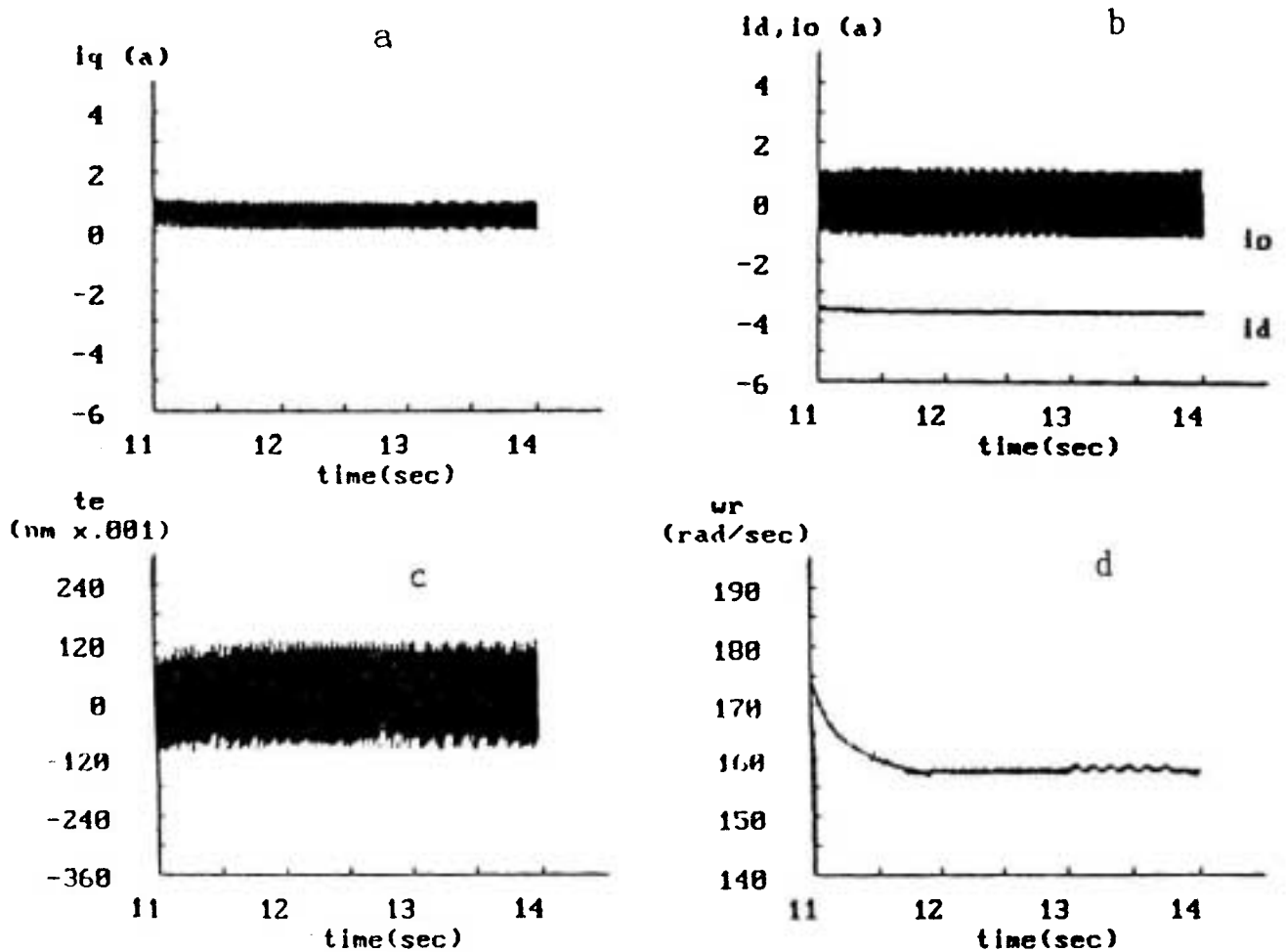


Figure 8. Steady-state on load performance of the machine for a sinusoidal-wave excitation voltage.



Figure 9. On load input voltage when load applied at $t=11$ seconds.

the final results. The reason is the lack of control system of the sinusoidal wave and consequently impossibility of adjusting the speed and presence of the 6th harmonic current within the motor.

REFERENCES

1. I. E. D. Pickup and D. Tipping, "Method for Predicting the Dynamic Response of a Variable Reluctance Stepping Motor", *Proc. IEE*, Vol. 120, No. 7, (July 1973), pp. 757-764.
2. M. R. Harris, et al.: "Unifying Approach to the Static Torque Stepping Motor Structures", *Proc. IEE*, Vol. 124, No. 12, (Dec. 1977), pp. 1215-1224.
3. J. M. Stephenson and J. Corda, "Computation of Torque and Current in Doubly-Salient Reluctance Motors from Nonlinear Magnetisation Data", *Proc. IEE*, Vol. 126, No. 5, pp. 393-396.
4. J. W. Finch, H. M. B. Metwally and J. A. Agber, :

"Performance Prediction in Saturated Variable Reluctance and Hybrid Motors", *Proc. IEE Conf.*, PEVD'90, London, pp. 231-236.

5. D. J. Kish, "The dq Analysis of a Variable Reluctance

Stepper Motor", M. Sc. Dissertation, University of Purdue, (1989).

6. P. C. Krause, "Analysis of Electric Machinery", *IEEE Press*, (1992).